

# Absorption, fluorescence, and Raman spectra of mass-selected rhenium dimers in argon matrices

Zhendong Hu, Jian-Guo Dong, John R. Lombardi, and D. M. Lindsay  
*Department of Chemistry and Center for Analysis of Structures and Interfaces (CASTI),  
The City College of New York (CCNY), New York, New York 10031*

W. Harbich  
*Institut de Physique Expérimentale, EPFL, CH-1015 Lausanne, Switzerland*

(Received 17 February 1994; accepted 21 March 1994)

We report absorption, laser fluorescence, and Raman spectra for  $\text{Re}_2$  in an argon matrix prepared by the mass-selected ion deposition technique. The dirhenium absorption spectrum consists of seven band systems (A–G) extending from the near infrared into the ultraviolet region. For the A system (a simple vibrational progression), we find  $T_0 = 10\,817(1)\text{ cm}^{-1}$ ,  $\omega_e = 317.1(5)\text{ cm}^{-1}$  and  $\omega_e x_e = 1.0(1)\text{ cm}^{-1}$ . A Franck–Condon analysis of the A system intensities predicts that this state has a smaller equilibrium internuclear distance than the ground state ( $\Delta r_e = -0.073\text{ \AA}$ ), in violation of Badger’s rule. The B system starts at  $13\,250\text{ cm}^{-1}$  and consists of four overlapping (and possibly perturbed) subsystems, whose average vibrational spacing is  $270(11)\text{ cm}^{-1}$ . The C, D, E, and F systems (vibrational spacings in parentheses) are centered at  $22\,300\text{ cm}^{-1}$  ( $210\text{ cm}^{-1}$ ),  $24\,500\text{ cm}^{-1}$  ( $195\text{ cm}^{-1}$ ),  $29\,150\text{ cm}^{-1}$  ( $175\text{ cm}^{-1}$ ), and  $32\,900\text{ cm}^{-1}$  ( $160\text{ cm}^{-1}$ ), respectively. Weak fluorescence spectra, obtained upon laser excitation into the A system, were characterized by vibrational progressions to the dimer ground ( $X$ ) state and to a low lying ( $X'$ ) state for which  $T_0 = 357.6(5)\text{ cm}^{-1}$  and  $\omega_e = 332.3(2)\text{ cm}^{-1}$ . Raman and fluorescence progressions to the ground state were observed when the B system was excited. These data give  $\omega_e = 337.9(49)\text{ cm}^{-1}$  for the dimer ground state in good agreement with measurements from photodetachment spectra [J. Am. Chem. Soc. **108**, 178 (1986)]. We propose likely assignments for the low lying electronic states of  $\text{Re}_2$  and discuss our results in terms of the bonding in the other group VIIB dimers,  $\text{Mn}_2$  and  $\text{Tc}_2$ .

## I. INTRODUCTION

Rhenium occupies a special position in inorganic chemistry, as  $[\text{Re}_2\text{Cl}_8]^{2-}$  is the first compound for which multiple metal–metal bonding was firmly established. In 1965, Cotton and Harris showed that the dirhenium bond length in  $[\text{Re}_2\text{Cl}_8]^{2-}$  was  $2.24\text{ \AA}$ , far shorter than the interatomic distance ( $2.75\text{ \AA}$ ) in the bulk metal.<sup>1–3</sup> It was quickly realized that this implied a strong overlap between the  $d$  orbitals of the two rhenium atoms. In what has now become a paradigm, it was proposed that the molecular orbitals arising from this interaction follow the energy ordering:  $d\sigma_g < d\pi_u < d\delta_g < d\delta_u^* < d\pi_g^* < d\sigma_u^*$ .<sup>4</sup> Placing eight electrons in this level scheme (Re is in a +3 oxidation state) gives rise to a  $d\sigma_g^2 d\pi_u^4 d\delta_g^2$  configuration. Thus  $[\text{Re}_2\text{Cl}_8]^{2-}$  possesses a quadruple bond, i.e., the dirhenium moiety has a formal bond order of 4.

Unligated metal dimers differ from their ligated cousins in several important aspects. The oxidation states in the former are zero, so that more electrons (14 in the case of  $\text{Re}_2$ ) are involved in the bonding. In addition, the  $s\sigma_g$  and  $s\sigma_u^*$  orbitals lie lower in energy and are generally at least partially filled. As a consequence of these two effects, metal dimers can have even stronger bonds than those in ligated species. For example,  $\text{Mo}_2$  has a  $d\sigma_g^2 d\pi_u^4 d\delta_g^4 s\sigma_g^2$  configuration and a bond length of  $1.93\text{ \AA}$  which is far shorter than in any ligated dimolybdenum species.<sup>2,3,5</sup>

In this paper, we present absorption, fluorescence, and Raman spectra for (unligated) rhenium dimers in argon matrices. As in several previous studies,<sup>6–10</sup> the dimer cation

(produced by sputtering) was mass selected in a Wien filter and then codeposited with argon and low energy electrons on a cold ( $\approx 14\text{ K}$ )  $\text{CaF}_2$  substrate. Aside from the ease of assigning spectral features, our (near) monodispersed matrix samples permit us to study dimer transitions with little or no overlap from any other (e.g., atomic) species. The dirhenium absorption spectrum is extraordinary in that seven band systems (some of which involve more than a single electronic state) are observed in the range  $\approx 200\text{--}1000\text{ nm}$ . All but one of these systems show vibrational structure. Linewidths in the red and infrared regions are sufficiently narrow (ca.  $20\text{ cm}^{-1}$ ) that full vibrational analyses were possible. Raman and fluorescence spectra, obtained by exciting into the red and infrared bands, give vibrational constants for two further states: The dimer ground state (for which we find  $\omega_e = 337.9 \pm 4.9\text{ cm}^{-1}$ , in good agreement with the previously measured value<sup>11</sup> of  $340 \pm 20\text{ cm}^{-1}$ ) and a low lying state whose electronic term energy is  $T_0 = 357.6 \pm 0.5\text{ cm}^{-1}$ . A total of 17 electronic states (including three observed previously)<sup>11</sup> have now been identified and (at least in part) analyzed, making dirhenium one of the best characterized transition metal dimers.

## II. EXPERIMENT

The CCNY cluster deposition source has been described in detail previously<sup>6,7</sup> so that only a brief description of the experimental arrangement will be given here. Clusters were produced by sputtering a rhenium target (Rembar, 99.97%) with an argon ion beam (typically  $15\text{ mA}$  at an energy of  $25$

keV) from a CORDIS ion source. Secondary ions were extracted with a modified Colutron model 200-B lens system and then mass-selected with a Wien filter (Colutron 600-B) in conjunction with a 175 mm drift space and 6.5 mm aperture. The dimer ion beam was bent by  $10^\circ$  to separate out neutral species and then guided towards the deposition region which consists of a cooled (approximately 14 K)  $\text{CaF}_2$  substrate surrounded by a "Faraday cage." The secondary ion beam line (extraction lens, Wien filter, etc.) was floated at about  $-1500$  V. Rhenium dimer ions were codeposited with the matrix gas (argon, from a coaxial injector ring) and low energy electrons (for neutralization) from a tungsten filament. Matrices were grown at  $4 \mu\text{h}$  with an argon:dimer ratio of approximately 5000:1. The dimer deposition energy is determined by the difference in potential between the sputtering target and the Faraday cage and was about 10 eV for the experiments described here. Ion currents could be measured on a Faraday plate situated in the deposition region. Typical ion currents (at 10 eV, optimized on the dimer) were 100 nA for  $\text{Re}_2^+$  with 100 and 20 nA for  $\text{Re}^+$  and  $\text{Re}_3^+$ , respectively. No absorption signal was observed when  $\text{Re}_2^+$  was deposited without electrons, indicating that the spectra reported below arise from the neutral dimer species. Fragmentation may be estimated by comparing the intensities of atomic excitation features in a dimer deposition with those obtained from depositions of the atom under similar conditions. By this measure we estimate the fragmentation of rhenium dimers (neutral bond energy,  $4 \pm 1$  eV)<sup>12</sup> to be  $15 \pm 5\%$ , which is considerably larger than the 1%–2% values found by us for other third row transition metal dimers.<sup>8–10</sup>

Matrix samples were interrogated *in situ* by absorption, resonance Raman, laser fluorescence and (only useful for detecting atomic rhenium) excitation spectroscopy. For both the absorption and excitation spectra, we employed a broadband (deuterium or tungsten) light source dispersed by a 1/4 m monochromator and then focused onto the matrix sample.<sup>6,13</sup> Absorption (and atomic excitation) spectra were recorded by observing the light scattered at right angles to the matrix surface, as described in more detail elsewhere.<sup>7,8</sup> This technique (which we term scattering depletion spectroscopy) relies on the depletion of scattered intensity by absorbing species in the matrix. Scattering depletion spectra (SDS) were acquired by taking the ratio of the scattered light (as a function of wavelength) from a region of the sample which is cluster poor (the reference intensity, generally near an edge) to that where the absorption is a maximum (the signal intensity).

Raman and fluorescence spectra were recorded using an argon ion laser (Spectra Physics model 2045) pumping either a dye laser (Coherent CR 599, with rhodamine 6G and DCM as dyes) or a titanium sapphire (TiS) laser (Lexel model 479). Typical fluences were 25–50 mW focused down to an estimated  $50 \mu\text{m}$  spot size. The exciting laser line was generally pre-dispersed with a grating in order to minimize fluorescence from the dye or TiS crystal. Light scattered at  $90^\circ$  was collected using  $f/1$  optics, focused onto a double 1/4 m monochromator and then detected using either a Hamamatsu R943-02 photomultiplier tube (PMT) or a silicon diode detector and photon counting techniques. The diode detector

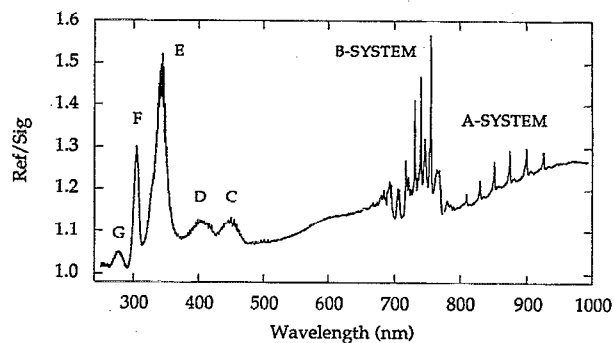


FIG. 1. Absorption (scattering depletion) spectrum of  $\text{Re}_2$  in an argon matrix. The spectrum was assembled in three segments (see text). The dimer content is approximately 350 nA h (Ref. 15).

(sensitive even beyond 1000 nm) was a "single photon counting module" (SPCM-200-PQ from General Electric Canada) and was specially selected to have a dark count of only 4 Hz. This unit (which directly outputs TTL pulses) was mounted on the exit plane of the monochromator, inside a light tight box accompanied by focusing optics which allowed alignment of the Raman signal with the approximately  $100 \mu\text{m}$  active area of the detector. Since the diode was anti-reflection (AR) coated at 630 nm, spectral measurements in the near infrared (NIR) were severely degraded by interference fringes arising from the silicon wafer itself. Accordingly, a second SPCM module, AR coated at 900 nm but with a 300 Hz dark count, was used for recording absorption (or other broadband) spectra beyond about 800 nm. Great care was taken in calibrating (with Hg spectra in first and second order) both the single and double 1/4 m monochromators, especially following any change of grating.

### III. SPECTRA AND ANALYSIS

Figure 1 shows the absorption (scattering depletion) spectrum of rhenium dimers in an argon matrix. The spectrum (of the unannealed sample) is assembled in three segments but has a common ordinate scale. Spectra between 250 and 290 nm were recorded with a deuterium lamp, but a tungsten lamp was used at longer wavelengths. The detector

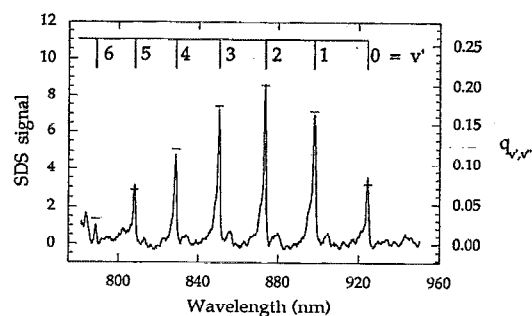


FIG. 2. Detail of the dirhenium A-system absorption bands after background subtraction. Superimposed dashed marks are calculated Franck-Condon factors (right-hand scale) for  $\Delta r_e = -0.073 \text{ \AA}$ . See text.

TABLE I. Absorption and emission frequencies for the A system of dirhenium in Ar. Notation is  $\Delta v = v' - v$ , where  $v, v'$  refer to the A and  $X'$  state, respectively. Column 4 entries denote pumped A-state level. Values in parentheses are calculated (see text). Units are  $\text{cm}^{-1}$ .

Band $v'$	Absorption frequency	Excitation frequency	Emission frequency from A-state level to state $X'$						
			Level $v'$	$\Delta v=5$	$\Delta v=4$	$\Delta v=3$	$\Delta v=2$	$\Delta v=1$	$\Delta v=0$
6	12 677	12 683							
5	12 372	12 370	5	12 012	11 681	(11 350)	11 012	10 685	(10 353)
5			4		11 697	11 362	11 031	10 705	(10 378)
4	12 065	12 062	4		11 708	11 373	11 041	10 715	(10 378)
4			3			11 393	11 056	10 733	10 407
3	11 756	11 752	3			11 414	11 075	10 731	10 407
3			2				(11 088)	10 768	10 433
2	11 446	11 446	2				(11 088)	10 770	10 433
1	11 132	11 136							
0	10 817								

in the region 250–775 nm was a PMT, whereas further to the red the Si diode detector noted above was employed. The segments correspond to two separate depositions (of about 4 h duration each),<sup>14</sup> the total dimer content of each sample being approximately 350 nA h.<sup>15</sup> The total acquisition time for Fig. 1 (spectral resolution 0.5–1 nm) was about 4 h.

The seven band systems observed for dirhenium (Fig. 1) have been labeled A–G, a choice of notation not meant to preclude still lower lying states. Indeed, Leopold *et al.* have analyzed a band system at 890  $\text{cm}^{-1}$  and report two other states centered around 5100 and 6200  $\text{cm}^{-1}$ .<sup>11</sup> Our absorption data begin at 10 000  $\text{cm}^{-1}$  with several relatively well resolved bands (labeled A and B) throughout the red and near infrared regions. The linewidths in the A and B systems (ca. 20  $\text{cm}^{-1}$ ) are surprisingly narrow. Four somewhat less resolved bands (labeled C, D, E, and F) appear in the ultraviolet. On closer inspection, these also show fairly sharp vibrational structure. No vibrational structure was observed in the G system, which is centered at around 277 nm. The A system consists of a series of almost equally spaced lines, while the B system is more irregular (possibly because of perturbations) but can be accounted for by four distinct progressions, each having approximately the same vibrational interval. We will also examine fluorescence and Raman spectroscopy observed by resonance excitation into various components of the A and B systems. Finally we discuss the ultraviolet bands, although these are less easily characterized and require further analysis which we will present in a future article.

### A. The A system

The A system consists of a simple vibrational progression shown more clearly in Fig. 2. Each of the observed bands is blue degraded due at least in part to (unannealed) matrix site effects. Thus, two weaker progressions (shifted to higher energy by 27 and 91  $\text{cm}^{-1}$ ) appeared after the sample was annealed at 30 K. The A-system progression terminates rather abruptly at 924.2 nm, which can therefore be identified as the origin ( $T_0$ ) for this transition. This permits an absolute numbering of the upper state vibrational quantum number ( $v'$ ), as indicated in Fig. 2. The measured positions (vacuum wavenumbers, estimated error  $\pm 2 \text{ cm}^{-1}$ )<sup>16</sup> of the A-system

transitions are given in Table I. A quadratic least squares fit (one standard deviation uncertainty in parentheses) to these data gives  $T_0 = 10\,817.0 (5) \text{ cm}^{-1}$ , with  $\omega_0 = 316.1 (4) \text{ cm}^{-1}$  and  $\omega_0 x_0 = 1.0 (1) \text{ cm}^{-1}$ .

The rather extensive progression observed for the A system suggests that the change in equilibrium internuclear distance between the ground state and the A state ( $\Delta r_e = r'_e - r''_e$ ) is fairly large. This change in internuclear distance was estimated by comparing the measured A-system intensities to those calculated assuming a harmonic oscillator potential for the lower state and a displaced anharmonic potential for the upper state. Apart from  $\Delta r_e$ , the two potentials are completely determined from the experimental vibrational constants given in Table II.<sup>17,18</sup> Calculated intensities were taken to be proportional to Franck–Condon factors ( $q_{v',v''}$ ) which were computed from overlap integrals (evaluated analytically)<sup>19</sup> between a harmonic oscillator wave function ( $v''=0$  for the  $X$  state) and excited state vibrational wave functions each represented by a sum of harmonic oscillator wave functions. The mixing coefficients for these sums were determined by perturbing (to first order) the harmonic oscillator potential ( $1/2 kx^2$ ) with a term  $\beta x^3 + \gamma x^4$ , where  $\beta$  and  $\gamma$  were obtained from the experimental  $\omega'_e$  and  $\omega_e x'_e$  using interrelationships between the vibrational constants and the parameters which define a Morse potential.<sup>17,18</sup> The agreement between the measured and calculated intensities (deter-

TABLE II. Spectroscopic constants for dirhenium, including band origins ( $X'$ , A, and B states) or centers (C–G systems) and force constants ( $k$ ). Estimated errors (see text) in parentheses.

State or system	$T_0$ ( $\text{cm}^{-1}$ )	$\omega_e$ ( $\text{cm}^{-1}$ )	$\omega_e x_e$ ( $\text{cm}^{-1}$ )	$k$ ( $\text{mdyne}/\text{\AA}$ )
X	0	337.9(47)	0.1(7)	6.26(17)
$X'$	357.6(5)	332.3(2)		6.06(1)
A	10 817(1)	317.1(5)	1.0(1)	5.52(2)
BI	13 251(14)	281(14)		4.0(3)
C	22 300	210(10)		2.4(2)
D	24 500	195(10)		2.1(2)
E	29 150	175(20)		1.7(4)
F	32 900	160(20)		1.4(4)
G	36 100			

mined using a simplex algorithm) was best for  $\Delta r_e = -0.073$  (2) Å, where the  $\pm 0.002$  Å error was determined by varying  $\Delta r_e$  near its optimum value until the difference (as judged by eye) between the calculated and measured intensities became conspicuous. Our best fit Franck–Condon factors are superimposed on the experimental A-system spectrum in Fig. 2.

The Franck–Condon analysis predicts  $r'_e < r''_e$  and thus (since  $\omega'_e < \omega''_e$ ) the A system violates Badger's rule,<sup>17</sup> which requires an inverse relationship between the internuclear distance and the vibrational frequency. Since this result is surprising (but not without precedent)<sup>20</sup> we also compared the measured intensities with those calculated for (a)  $\Delta r_e > 0$  and (b) for situations where the electronic transition moment,  $R_e(r)$ , was not assumed to be constant. The simplex fit to the experimental intensities also found a local (but not global) minimum for  $\Delta r_e = +0.084$  Å. If the potentials for both the X and A states were assumed to be harmonic, then the optimum  $\Delta r_e$  was  $\pm 0.076$  Å. In both cases, however, the comparison between the measured and calculated intensities was decidedly inferior to that shown in Fig. 2. Relative intensities in absorption depend not only upon  $q_{v',v''}$ , but are proportional to the product  $q_{v',v''} R_e^2(r)$ ,<sup>17</sup> where  $R_e(r)$  depends upon the upper state vibrational level and might change significantly over the range  $v'' = 0 \rightarrow 6$ .<sup>21</sup> In the absence of an independent determination of  $\Delta r_e$  (as could be obtained from a rotational analysis of the gas-phase spectra), there is no *a priori* means of determining the vibrational dependence of  $R_e(r)$ . In order to explore the sensitivity of our calculated  $\Delta r_e$  values to changes in  $R_e(r)$ , we arbitrarily set this function equal to 1.0, 1.2, 1.4, ..., 2.2 for  $v'' = 0, 1, 2, \dots, 6$  and then reoptimized the A-system intensity data. The best fit  $\Delta r_e$  remained negative, changing in magnitude by approximately 0.01 Å. Accordingly, we feel that  $r'_e < r''_e$  is indeed likely, unless  $R_e(r)$  depends upon  $v''$  in some manner which alters this result.

Six of the A-system bands ( $v' = 1$  through 6) were excited by an argon ion pumped TiS laser and the resulting emission was recorded (using a Si diode detector) with a resolution of approximately  $10 \text{ cm}^{-1}$ . Representative spectra are shown in Figs. 3(a) and 3(b) for  $v' = 5$  and 4, respectively. Except for  $v' = 1$  and 6, which show no recognizable dimer features, the emission spectra are characterized by two fluorescence progressions, one from the pumped A-system level and a second from the vibrational level immediately below it, to a low lying excited state denoted  $X'$  plus a third (also fluorescence) progression from levels  $v' - 1, v' - 2$ , etc. of the A system terminating in  $v'' = 0$  of the dimer ground (X) state. In Fig. 3, these features are labeled  $X'SP(v')$  and  $X'SP(v' - 1)$  for the two  $X'$  state progressions and ASP for the A-system progression; the label  $v$  refers to vibrational levels of the  $X'$  state. None of the features marked in Fig. 3 (except that from the  $\text{CaF}_2$  support)<sup>22</sup> correspond to Raman spectra, as they occur at the same absolute energies when the excitation wavelength is shifted slightly (typically,  $25\text{--}50 \text{ cm}^{-1}$ ) off resonance. Table I lists measured emission frequencies for the two progressions  $X'SP(v')$  and  $X'SP(v' - 1)$ . In this table, the pumped level is given in column 1, the corresponding emitting levels are listed in col-

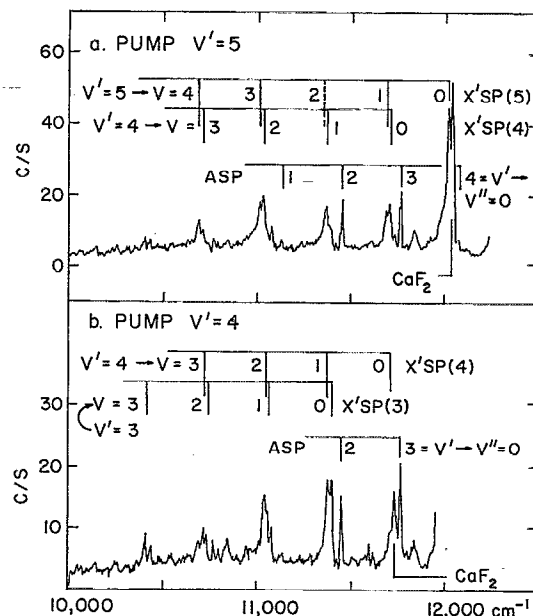


FIG. 3. Dirhenium fluorescence spectra resulting from laser excitation of the A system  $v' = 5$  and 4 bands. The labels  $v$  and  $v''$  pertain to the  $X'$  and X states, respectively. ASP and  $X'SP$  refer to A- and  $X'$ -state progressions (see text). Both panels have the same energy scale.

umn 4 and the emission frequencies are grouped according to  $\Delta v = v' - v$ . Values in parentheses were calculated using the spectroscopic constants given below. The frequencies measured for the vibrational progression (ASP) to  $v'' = 0$  of the ground state are not included in Table I, as these data agree remarkably well (generally to better than  $5 \text{ cm}^{-1}$ ) with the positions of the absorption maxima given in column 2 of this table. The energies of the  $X'$  state vibrational levels were obtained from the difference between the energy of the emitting level (column 2 data) and the fluorescence frequencies in columns 5–10. The average values obtained (one standard deviation uncertainty in parentheses) are  $358(5)$ ,  $689(9)$ ,  $1022(8)$ ,  $1355(6)$ , and  $1687 \text{ cm}^{-1}$  for  $v = 0\text{--}4$ , respectively. A linear least squares fit to these data gave  $T_0 = 357.6 \pm 0.5 \text{ cm}^{-1}$  with  $\omega_0 = 332.3 \pm 0.2 \text{ cm}^{-1}$ . Since the uncertainties in these constants are considerably smaller than those in the positions of  $v = 0\text{--}4$ , a more reasonable set of errors for  $T_0$  and  $\omega_0$  is  $\pm 2 \text{ cm}^{-1}$  and  $\pm 1 \text{ cm}^{-1}$ , respectively.

## B. The B system

The B system, which extends from 650 to 800 nm as shown in Fig. 4, is considerably more complicated than the A system. Although at first sight the spectrum appears to be totally irregular, most of the B system features can be separated into four subsystems (labeled I–IV) each containing some 3–5 approximately equally spaced transitions. As discussed below, fluorescence spectra recorded after pumping various transitions of the B system all result in emission from  $v' = 0$  of subsystem I, which implies that B-system dimers relax to this lowest vibrational level before emitting to the ground state. Accordingly, the absolute origin of sub-

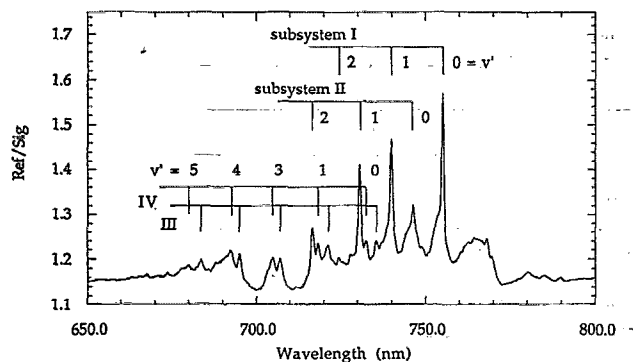


FIG. 4. Detail of the dirhenium B-system absorption bands, showing assignment to subsystems I–IV.

system I can be assigned as the prominent feature shown in Fig. 4. It also seems likely that the origin of subsystem II is the feature labeled  $v' = 0$ , but the absolute numbering of the remaining subsystems (III and IV) is less certain. Table III gives vibrational term energies (measured from the absorption spectra) relative to  $v' = 0$  of subsystem I, for which  $T_0 = 13251 \pm 14 \text{ cm}^{-1}$ . The relatively large error ( $\pm 14 \text{ cm}^{-1}$ ) in  $T_0$  results from uncertainties in measuring *absolute* wavelengths and was estimated by averaging absorption data from three different dirhenium depositions. By contrast, the uncertainties (ca.  $\pm 2 \text{ cm}^{-1}$ ) in *relative* wavelength values (as pertain to the Table III data) are much less. The mean vibrational intervals for subsystems I–IV are  $281(14) \text{ cm}^{-1}$ ,  $276(15) \text{ cm}^{-1}$ ,  $258(17) \text{ cm}^{-1}$ , and  $265(6) \text{ cm}^{-1}$ , respectively. The large uncertainties (given in parentheses) in these frequencies suggests that the B-system levels are perturbed, perhaps by the A state as is suggested by the emission data described in the following paragraph and by the dirhenium potential curves discussed in Sec. V. The grouping of subsystems I–IV into a narrow (ca.  $2000 \text{ cm}^{-1}$ ) energy region and the similarity in their vibrational frequencies (average value:  $270 \pm 11 \text{ cm}^{-1}$ ) suggests that subsystems I–IV are somehow related. For example they might be different multiplets of the same electronic state, or (see Ref. 17 and Sec. IV) be levels grouped by an  $(\omega, \omega)$  coupling scheme. However, the *intensities* (which depend upon the  $\Delta r_e$  values) of subsystems I–IV indicate that this is not the case. In order to explore this aspect, we performed a Franck–Condon analysis on subsystems I and II in a manner similar to that described

TABLE III. B-system term energies (relative to  $v' = 0$  of subsystem I) measured from the absorption spectrum of dirhenium in argon. Notation corresponds to that used in Fig. 4. Units are  $\text{cm}^{-1}$ . Estimated uncertainties (see text)  $\pm 2 \text{ cm}^{-1}$ .

Subsystem	B-system vibrational level ( $v'$ )				
	0	1	2	3	4
I	0	271	563		
II	160	446	711		
III	356	624	901	1147	1387
IV	410	680	945	1201	1468

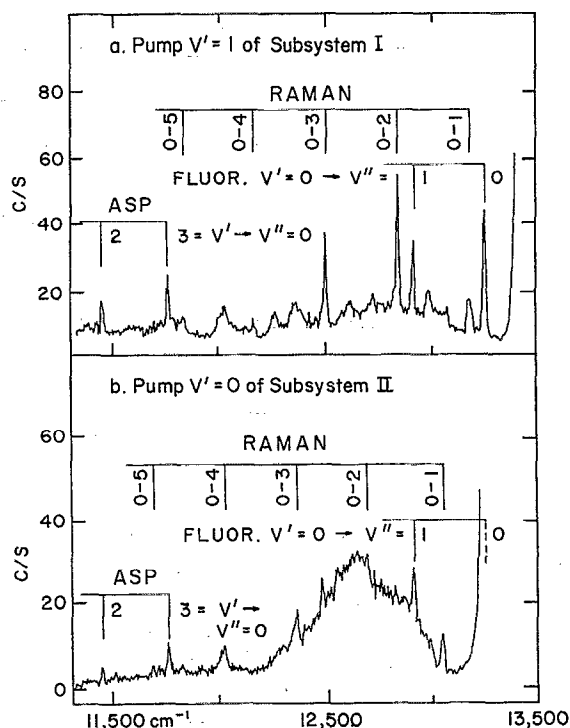


FIG. 5. Representative Raman and fluorescence spectra resulting from laser excitation of the dirhenium B system. The labels  $v'$  and  $v''$  pertain to the B and X states, respectively. ASP denotes A-state progression (see Fig. 3 and text). Both panels have the same energy scale.

for the A system above. Experimental intensities were taken to be proportional to peak heights and harmonic oscillator potentials were used for both the lower and upper states. This analysis gave  $\Delta r_e = \pm 0.040 \text{ \AA}$  and  $\Delta r_e = \pm 0.059 \text{ \AA}$  for subsystems I and II, respectively. Although preliminary, these results do imply that these two subsystems are more different in character than their vibrational frequencies would suggest.

Five of the B-system bands were excited at 32 different wavelengths ( $\text{Ar}^+$  pumped Ti:S laser) both on and slightly off ( $\leq 50 \text{ cm}^{-1}$ ) resonance of the  $v' = 0, 1, 2$  transitions of subsystems I and II and  $v' = 2$  and 3 for subsystems III and IV. Representative spectra (recorded at  $10 \text{ cm}^{-1}$  resolution) are shown in Figs. 5(a) and 5(b). The spectra for subsystems I and II were characterized by both Raman and fluorescence progressions, whereas those obtained by pumping subsystems III and IV gave only fluorescence. The Raman spectra all pertain to the dirhenium ground state. Table IV gives the average Stokes shifts derived from the subsystem I and II measurements (13 wavelengths each), with estimated uncertainties (one standard deviation) in parentheses. The fluorescence spectra, by contrast, are of two types. One fluorescence progression (denoted ASP in Fig. 5) consisted of emission from vibrational levels  $v' = 3, 2$ , etc. of the A system to  $v'' = 0$  of the ground state and is similar in character to that discussed in Sec. III A, above. A second fluorescence progression consisted of emission from the  $v' = 0$  level of subsystem I to levels  $v'' = 0, 1$ , etc. of the ground state and was observed regardless of which B-system level that was

TABLE IV. B-state emission data giving ground state intervals for dirhenium in Ar. The notation R and F refers to Raman and fluorescence measurements, respectively. Estimated errors in parentheses. Units are  $\text{cm}^{-1}$ .

Pump subsystem	Emission type	$T_0$ for B state	Ground state interval				
			0-1	0-2	0-3	0-4	0-5
I	R	13,252(6)	334.7(43)	674.8(37)	1013.8(24)	1351.2(21)	1682.6
	F		335.5(58)	678.1(81)			
II	R	13,256(5)	327.5(58)	674.7(48)	1012.9(68)	1349.4(23)	1692.5(96)
	F		337.0(51)	686.4(94)	1013.1(131)		
III/IV	F	13,258(4)	337.5(38)				
Averages ( $\pm\sigma$ )		13255(3)	334.4(40)	678.5(55)	1013.3(5)	1350.3(13)	1687.6(70)

pumped i.e., excited B-system molecules relax to their (presumed lowest) energy level ( $v'=0$  of subsystem I) before emitting. The fluorescence spectra were also used to obtain ground state vibrational intervals and the Table IV data are averages (uncertainties in parentheses) of 13 measurements each for subsystems I and II and three measurements for each of subsystems III and IV. The fluorescence data (column 3 of Table IV) also give a value for the electronic term energy for the B state,  $T_0 = 13\,255 \pm 3 \text{ cm}^{-1}$ , in good agreement with that obtained from the absorption measurements. Ground state vibrational constants were obtained using an average of both the fluorescence and Raman data (last row in Table IV). A least squares fit to these vibrational data gives  $\omega_e'' = 337.9 \pm 4.7 \text{ cm}^{-1}$ , with  $\omega_e x_e'' = 0.1 \pm 0.7 \text{ cm}^{-1}$ .

### C. The C, D, E, F, and G systems

The dirhenium "ultraviolet bands" consist of five systems (C–G) four of which are shown in more detail in Fig. 6. All four systems show vibrational structure, as indicated by the "stick spectra" in this figure. In order to make this structure apparent, the vertical scale for the (weaker) C and D systems has been enlarged approximately fourfold with respect to that for the E and F systems. True relative intensities can be determined from Fig. 1; the wavelength scale in Fig. 6 is the same for all four systems. While the E and F systems show a single vibrational progression each, both the C and D systems consist of several overlapping progressions the most prominent of which have been labeled subsystems I and II in

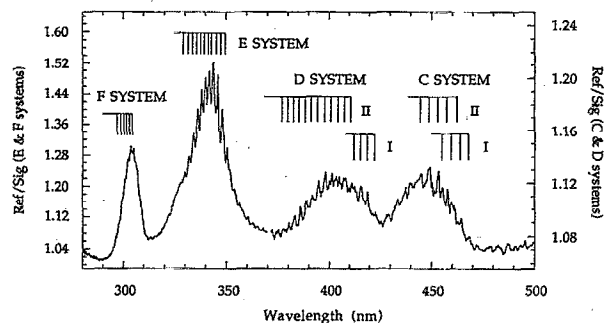


FIG. 6. Detail of the dirhenium ultraviolet bands. Most C and D system features are assigned to two subsystems, labeled I and II. Note that for clarity the E, F systems (left hand axis) and C, D systems (right-hand axis) have different scales.

Fig. 6. When examined in detail, the C and D systems are seen to consist of more than two "subsystems" each, but for these no more than two or three transitions could be positively identified. Measured positions for the vibrational transitions of the ultraviolet bands are given in Table V. The origins of each progression (i.e., absolute numberings) are uncertain and may well lie several vibrational quanta to higher wavelengths than indicated in either Fig. 6 or Table V. The measured vibrational frequencies (average spacings  $\pm 1$  standard deviation) are  $204 \pm 13 \text{ cm}^{-1}$  and  $215 \pm 9 \text{ cm}^{-1}$  for subsystems I and II of the C system,  $193 \pm 9 \text{ cm}^{-1}$  and  $197 \pm 13 \text{ cm}^{-1}$  for subsystems I and II of the D system, and  $176 \pm 21 \text{ cm}^{-1}$  plus  $161 \pm 21 \text{ cm}^{-1}$  for the E and F systems, respectively. These data are collected in Table II together with approximate positions for the band centers, including that of the G system for which no vibrational structure was observed.

### IV. ASSIGNMENT OF THE DIRHENIUM SPECTRA

In this section we focus on possible assignments for the dirhenium ground and low lying excited ( $X'$ , A, and B) states. Apart from photodetachment spectra,<sup>11</sup> there is no published gas-phase (or other matrix) spectroscopy on  $\text{Re}_2$ . Since the low lying neutral dimer states observed by Leopold, Miller, and Lineberger<sup>11</sup> fall outside our spectral range, the matrix measurements overlap those from the pho-

TABLE V. Measured positions of vibrational bands in most prominent progressions of the dirhenium C, D, E, and F systems. The upper state assignment  $v'=0, 1, 2$ , etc. is relative. Transitions closest to band centers are italicized. Units are  $\text{cm}^{-1}$ .

$v'$	C system		D system		E system	F system
	I	II	I	II		
0	21 369	21 628	23 677	<i>24345</i>	28585	32827
1	21 558	21 855	23 880	24531	28774	32979
2	21 769	22 067	24 070	24719	28949	33121
3	21 980	22 283	24 257	24934	<i>29143</i>	33275
4		22 489		25129	29279	33442
5				25345	29443	33633
6				25553	29600	
7				25737	29768	
8				25944	29964	
9				26127	30145	
10				26319	30346	
11				26508		

todetachment experiments only in the determination of  $\omega_e''$ . As noted above, there is good agreement between the photo-detachment and matrix values for this parameter,  $\omega_e''=340\pm 20$  and  $338\pm 5$   $\text{cm}^{-1}$ , respectively. Apparently because of difficulties in handling relativistic effects, no molecular structure calculations have so far been attempted for dirhenium. We hope that our experimental results and tentative state assignments will motivate the theoretical community to try and overcome these calculational difficulties. The arguments to follow are based upon (a) bond dissociation energies, (b) the qualitative ideas developed by Cotton *et al.*<sup>2,3</sup> for  $d$  bonding in ligated metal clusters plus the correlation and state assignment schemes described in the seminal work by Herzberg,<sup>17</sup> all in combination with (c) many of the spectroscopic observations described above. The ensuing discussion follows this order.

### A. The bond strength of dirhenium

There is one further piece of information in addition to the results published here and in Ref. 11, namely evidence that the dirhenium bond dissociation energy,  $D(\text{Re}_2)$ , lies in the range 30 000–40 000  $\text{cm}^{-1}$ . Thus various semi-empirical treatments of thermodynamic data suggest  $D(\text{Re}_2)=4\pm 1$  eV.<sup>12</sup> Confirming this value is the absence of predissociation, at least to energies below 31 300  $\text{cm}^{-1}$ , in the gas-phase spectra of  $\text{Re}_2$ .<sup>23</sup> To proceed further, it is necessary to consider the atomic asymptotes which must correlate with any dimer electronic states. For transition metal diatomics in general,<sup>12,24,25</sup> chemical bond formation is most favorable in those instances where at least one of the interacting atomic moieties has an open  $s$ -shell configuration:  $s^1d^m$  as opposed to  $s^2d^{m-1}$ . If  $s^1d^m$  is not the ground state configuration, bonding can still take place but at the cost of a certain amount of “promotional energy”. If this prescription holds for rhenium,<sup>26</sup> where  $5d^56s^2(^6S_g)$  lies lowest with  $5d^66s^1(^6D_g)$  higher by approximately 14 000  $\text{cm}^{-1}$ ,<sup>27</sup> then the dimer ground state asymptote is likely to be  $5d^56s^2(^6S_g)+5d^66s^1(^6D_g)$  rather than  $5d^66s^1(^6D_g)+5d^66s^1(^6D_g)$  for which the promotion energy would be large, approximately 28 000  $\text{cm}^{-1}$ . Assuming that  $D_e=\omega_e^2/4\omega_e x_e$  is applicable to the dirhenium A state (e.g., it can be described by a Morse potential function),<sup>17</sup> then the Table II data give  $D_0(A)=25\,000\pm 2500$   $\text{cm}^{-1}$  as the spectroscopic dissociation energy for this state. Since the absorption spectra give  $T_0(A)=10\,817\pm 1$   $\text{cm}^{-1}$  for the electronic term energy of the A state, a dirhenium bond energy of  $4\pm 1$  eV requires that the A state dissociate to *two ground state atoms*, i.e.,  $5d^56s^2(^6S_g)+5d^56s^2(^6S_g)$ . In this situation, the spectroscopic dissociation energy for the X state is determined to be  $D_0(X)=49\,800\pm 2500$   $\text{cm}^{-1}$ , and the corresponding bond energy is  $D(\text{Re}_2)=35\,800\pm 2500$   $\text{cm}^{-1}$ . It is worth noting that the predicted ground state anharmonicity is therefore  $\omega_e x_e''=0.57(3)$   $\text{cm}^{-1}$ , which agrees with the (very uncertain) value  $(0.1\pm 0.7$   $\text{cm}^{-1})$  measured from the Raman spectra.

### B. Configurations and possible state assignments

In the following discussion, we adopt the “conventional” energy order for molecular orbitals arising from the overlap of atomic  $5d$  functions:  $d\sigma_g < d\pi_u < d\delta_g < d\delta_u^* < d\pi_g^* < d\sigma_u^*$ .<sup>2</sup> In addition, the  $6s$  functions give rise to  $s\sigma_g$  and  $s\sigma_u^*$  orbitals, where  $s\sigma_g$  undoubtedly lies below  $d\sigma_g$  and so can be assumed to be doubly occupied in all dirhenium configurations considered in this article. Depending upon the strength of the interaction between the  $s$ -orbitals, however, the  $s\sigma_u^*$  orbital might be doubly or singly occupied. The former case corresponds to “weak  $s$ -orbital overlap” (e.g.,  $s\sigma_u^*$  lies below  $d\sigma_g$ ), whereas the latter would arise if the  $s$ -orbital overlap were sufficiently strong to raise  $s\sigma_u^*$  to the region of the  $\delta$  orbitals. The case of an empty  $s\sigma_u^*$  orbital (i.e.,  $s\sigma_u^*$  lies even higher in energy) need not be considered as configurations derived from this occupancy would correlate asymptotically with two  $5d^66s^1(^6D_g)$  atoms.

Since we suppose that the dirhenium A state dissociates to two  $5d^56s^2(^6S_g)$  atoms, this should arise from a configuration in which both  $s\sigma_g$  and  $s\sigma_u^*$  are doubly occupied. Two reasonable candidates are  $s\sigma_g^2s\sigma_u^{*2}d\sigma_g^2d\pi_u^4d\delta_g^4$ , corresponding to  $^1\Sigma_g^+(0_g^+)$ , and  $s\sigma_g^2s\sigma_u^{*2}d\sigma_g^2d\pi_u^4d\delta_g^3d\delta_u$  which gives rise to  $^1\Sigma_u^+$ ,  $^3\Sigma_u^+$ ,  $^1\Gamma_u$ , and  $^3\Gamma_u$  of which only  $^3\Sigma_u^+$  ( $0_u^-$  and  $1_u$ ) can result from two separated atoms each in a  $^6S_g$  state.<sup>17</sup> In these configurations (as in those following) the exact position of  $s\sigma_u^*$  is not necessarily implied. Thus we do not distinguish between  $s\sigma_g^2s\sigma_u^{*2}d\sigma_g^2d\pi_u^4d\delta_g^4$  and (e.g.)  $s\sigma_g^2d\sigma_g^2s\sigma_u^{*2}d\pi_u^4d\delta_g^4$ , both of which correspond to a  $^1\Sigma_g^+$  state, although  $s\sigma_g^2s\sigma_u^{*2}d\sigma_g^2d\pi_u^4d\delta_g^4$  is (formally, at least) to be expected for states in which the  $s$ -orbital overlap is weak. In the dimer ground state configuration  $s\sigma_u^*$  should be singly occupied, as this state dissociates to  $5d^56s^2(^6S_g)+5d^66s^1(^6D_g)$ . Likely configurations for this situation are  $s\sigma_g^2d\sigma_g^2d\pi_u^4d\delta_g^4s\sigma_u d\delta_u$ , which will give rise to  $^1\Delta_g(2_g)$  and  $^3\Delta_g(3_g, 2_g, \text{ and } 1_g)$  states plus  $s\sigma_g^2d\sigma_g^2d\pi_u^4d\delta_g^4s\sigma_u d\pi_g$ , corresponding to  $^1\Pi_u(1_u)$  and  $^3\Pi_u(2_u, 1_u, \text{ and } 0_u^+)$ .<sup>17,28</sup> In Hund’s case (c), the  $\Delta$  and  $\Pi$  states group according to  $(\omega_1, \omega_2)$ , where  $\omega = \lambda + s$ , in which  $\lambda$  and  $s$  are one electron orbital and spin angular momenta.<sup>17</sup> Thus, in the absence of other perturbing states, the energy order for  $^3\Pi_u$  and  $^1\Pi_u$  is  $0_u^+(^3\Pi_u) < 1_u(^3\Pi_u) \ll 2_u(^3\Pi_u) < 1_u(^1\Pi_u)$ , where the splitting between  $(\omega_1, \omega_2)=(1/2, 1/2)$  and  $(3/2, 1/2)$  is approximately twice the spin-orbit coupling constant for a Re  $5d$  electron ( $2\zeta_{5d} \approx 5000$   $\text{cm}^{-1}$ ),<sup>27</sup> and the separation within each  $(\omega_1, \omega_2)$  pair is proportional to the exchange splitting (for which we have no estimate) between  $^3\Pi_u$  and  $^1\Pi_u$ .<sup>29</sup> A similar analysis pertains to the  $^1\Delta_g$  and  $^3\Delta_g$  states, so that  $1_g(^3\Delta_g) < 2_g(^3\Delta_g) \ll 3_g(^3\Delta_g) < 2_g(^1\Delta_g)$ .

### C. The dirhenium A and B systems

If the A state is assigned as  $^1\Sigma_g^+(0_g^+)$ , then (because of the  $g \leftrightarrow u$  selection rule) the X state must derive from  $\Pi_u$  and not  $\Delta_g$  i.e. our corresponding ground state assignment is  $0_u^+(^3\Pi_u)$  or (see below)  $1_u(^3\Pi_u)$ . As discussed in Sec. III, the A system fluorescence spectra show emission to two states (X and X'). Since both fluorescence progressions have

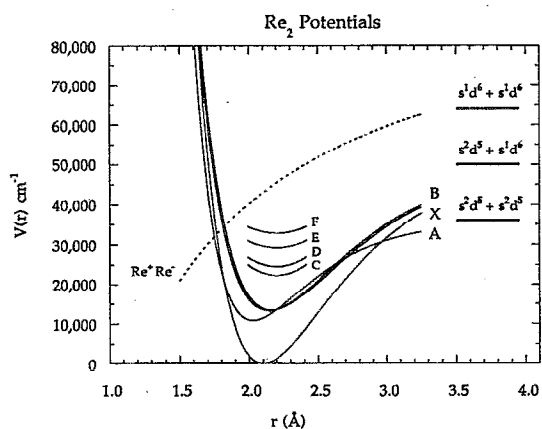


FIG. 7. Potential energy curves for eight dirhenium states.

“similar character” i.e. absolute intensities and Franck–Condon profiles, it is reasonable to suppose that the X and X' states have similar electronic structures. By contrast, the B system fluoresces to the X state only, so that (apparently) the B  $\rightarrow$  X' transition violates the  $\Delta\Omega=0, \pm 1$  selection rule for Hund's case (c).<sup>17</sup> These observations may be rationalized if  $1_u$  is the dirhenium ground state  $0_u^+$  is the X' state and the B system level at  $13\,252\text{ cm}^{-1}$  (i.e., the subsystem I origin) is assigned as a state (of unknown parentage) having  $2_g$  symmetry. This scheme requires a reversal in the normal energy order of  $0_u^\pm$  and  $1_u$ , but this might arise if  $1_u(3\Pi_u)$  were perturbed by another low lying state also of  $1_u$  symmetry. On the assumption that the A state derives from  $3\Sigma_u^+$ , similar reasoning leads to an assignment of  $1_g(3\Delta_g)$  as the ground state with X' as  $2_g(3\Delta_g)$ , the A state as  $1_u(3\Sigma_u^+)$ , and a B state having  $0_u^\pm$  symmetry but not necessarily corresponding to the other component of  $3\Sigma_u^+$ . Although this scheme does not invoke a perturbative reordering of the energy levels, the small ( $358\text{ cm}^{-1}$ ) separation between the X( $1_g$ ) and X'( $2_g$ ) states is not easily justified.

## V. DISCUSSION

A rather striking aspect of the spectroscopic data collected in Table II is the monotonic decrease in vibrational frequency with increasing electronic energy. If the experimental  $\omega_e$  are plotted against their corresponding electronic energies (band origins or band centers) all the data points with one exception (that for the A state) fall on or close to a smooth curve. This is perhaps an indication that the X–G (but not A) states correlate with the same asymptote, presumably  $5d^56s^2 + 5d^66s^1$ . The fact that the datum for the A state is exceptional is one further indication of its unusual character. As noted above, this state most likely dissociates to two ground state atoms and it also violates Badger's rule.

A visual summary of our dirhenium results is given in Fig. 7, which shows potential energy curves for eight dimer states. The X and A states are represented by Morse potentials parameterized by the vibrational constants and electronic term energies given in Table II, by an X-state dissociation energy of  $49\,900\text{ cm}^{-1}$ , as proposed in Sec. IV A,

and by the difference in internuclear separation ( $\Delta r_e = -0.073\text{ \AA}$ ) obtained from our Franck–Condon analysis. The atomic asymptotes for the X and A states are taken to be  $5d^56s^2 + 5d^66s^1$  and  $5d^56s^2 + 5d^66s^2$ , respectively. The absolute value of  $r_e''$  (which is unknown) was chosen to be  $2.1\text{ \AA}$ . This estimate was arrived at by using Pauling's rule<sup>30,31</sup> to extrapolate data (Fig. 8.1.1 in Ref. 2) for the variation in bond length with bond order in ligated  $\text{Re}_2$  clusters. Bond orders for the unligated dimer were computed for the electronic configurations discussed in Sec. IV B. This procedure gives formal bond orders of 4.5–5, corresponding to a Morse potential ( $\omega_e$  from Table II;  $\Delta r_e = +0.045\text{ \AA}$  from the Franck–Condon analysis), assuming that this state dissociates to the same asymptote as the ground state. A common origin ( $r_e = 2.2\text{ \AA}$ , arbitrary) was chosen for the C, D, E, and F states, which are drawn as harmonic oscillator functions ( $\omega_e$  values from Table II). The ionic ( $\text{Re}^+\text{Re}^-$ ) curve<sup>32</sup> has a value of  $45\,000\text{ cm}^{-1}$  at  $2.2\text{ \AA}$  and clearly has little influence on the covalent states. One aspect of Fig. 7 is its suggestion that the B- and A-state potentials approach each other and run parallel (perhaps intersecting) over a wide range ( $\approx 2.2\text{--}2.7\text{ \AA}$ ) of internuclear distances. This situation might well give rise to perturbations, which could be the origin of the irregular B system vibrational spacings noted earlier. A more quantitative assessment of this possibility requires a simulation (soon to be initiated) of the several overlapping subsystems in the B region. Simulations of the ultraviolet bands are also planned and, together with emission studies, these should provide better spectroscopic constants for the C, D, E, and F states.

Ground state force constants are now known for 23 of a possible 30 homonuclear transition metal dimers.<sup>33</sup> Since the dirhenium force constant ( $6.26\text{ mdyne/\AA}$ ) is second only to that found in  $\text{Mo}_2$  ( $6.43\text{ mdyne/\AA}$ ),<sup>5</sup> it is clear that this species does involve multiple metal–metal bonding. In fact, we suggested above that  $\text{Re}_2$  has a bond order of 4.5–5. This is in sharp contrast to the situation found for the third row congener ( $\text{Mn}_2$ ) which is best considered as a van der Waals molecule, i.e., as having a bond order of zero.<sup>34–36</sup> Both metals have  $s^2d^5$  ground state configurations and their  $s^1d^6$  configurations lie higher in energy by similar amounts ( $2.15$  and  $1.76\text{ eV}$  for Mn and Re, respectively).<sup>25</sup> Thus, the dramatic change in bonding character undoubtedly comes about because the  $5d$  orbitals of two Re atoms overlap more strongly than the  $3d$  orbitals of two Mn atoms. As discussed above and elsewhere,<sup>8,24,25</sup> strong overlap is favored in cases where the  $nd$  orbitals are diffuse relative to the  $(n+1)s$  orbitals. For rhenium,  $\langle r_{5d} \rangle / \langle r_{6s} \rangle = 0.570$  which is much larger than the corresponding ratio of expectation values,  $\langle r_{3d} \rangle / \langle r_{4s} \rangle = 0.351$  for Mn.<sup>25</sup> In this context, it is of interest to speculate on the bonding in  $\text{Tc}_2$  which, because of its cost and mild radioactivity, is unlikely to be studied in the near future. Atomic Tc also has a  $s^2d^5$  ground state configuration, but  $s^1d^6$  lies only  $0.41\text{ eV}$  higher.<sup>25</sup> Since the ratio of expectation values,  $\langle r_{4d} \rangle / \langle r_{5s} \rangle = 0.474$ ,<sup>17</sup> is intermediate between the corresponding values for Mn and Re, the  $4d$  dimer might well be relatively strongly bound. A further indication of the relative stability of  $\text{Tc}_2$  can be seen from bulk cohesive en-

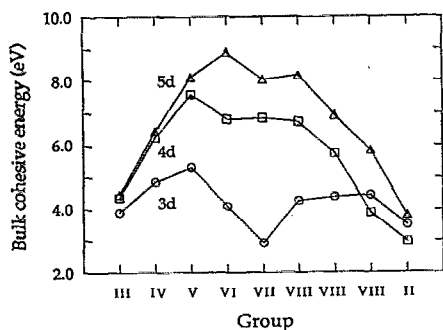


FIG. 8. Bulk cohesive energy data (Ref. 37) for 3d (circles), 4d (squares), and 5d (triangles) transition metals.

ergy data,<sup>37</sup> which we present graphically in Fig. 8. The cohesive energies of the third row metals dip sharply near Mn, but this phenomenon is absent or much less pronounced for the 4d and 5d elements, which suggests that Tc is closer to Re in its bonding than it is to Mn.

To recapitulate, we have identified and (in part) analyzed eight absorption and emission systems for dirhenium in argon. Including various "subsystems" (I, II, etc.) for the B, C, and D bands, we have obtained parameters for 14 electronic states in this molecule. Since photodetachment spectra have identified a further three band systems,<sup>11</sup> dirhenium can now be classified as one of the best characterized transition metal dimers.

## ACKNOWLEDGMENTS

We wish to thank Professor Michael Morse and Professor Robert Field for helpful and stimulating conversations. This work was supported by the National Science Foundation under Cooperative Agreement No. RII-9353488 and Grant No. CHE-9112897 and by the City University<sup>3</sup> of New York PSC-BHE Faculty Research Award Program.

<sup>1</sup>F. A. Cotton and C. B. Harris, *Inorg. Chem.* **4**, 330 (1965).

<sup>2</sup>F. A. Cotton and R. A. Walton, *Multiple Bonds Between Metal Atoms* (Wiley, New York, 1982).

<sup>3</sup>B. E. Bursten and W. F. Schneider, in *Metal-Metal Bonds in Chemistry and Catalysis*, edited by J. P. Fackler (Plenum, New York, 1990).

<sup>4</sup>F. A. Cotton, N. F. Curtis, C. B. Harris, B. F. G. Johnson, S. J. Lippard, T. G. Mague, W. R. Robinson, and J. S. Wood, *Science* **145**, 1305 (1964).

<sup>5</sup>Y. M. Efremov, A. N. Samoilova, V. B. Kozhukhovskiy, and L. V. Gurvich, *J. Mol. Spectrosc.* **73**, 430 (1978).

<sup>6</sup>Z. Hu, B. Shen, Q. Zhou, S. Deosaran, J. R. Lombardi, D. M. Lindsay, and W. Harbich, *J. Chem. Phys.* **95**, 2206 (1991).

<sup>7</sup>Z. Hu, B. Shen, Q. Zhou, S. Deosaran, J. R. Lombardi, and D. M. Lindsay, *Proc. SPIE* **1599**, 65 (1992).

<sup>8</sup>Z. Hu, B. Shen, J. R. Lombardi, and D. M. Lindsay, *J. Chem. Phys.* **96**, 8757 (1992).

<sup>9</sup>Z. Hu, J.-G. Dong, J. R. Lombardi, and D. M. Lindsay, *J. Chem. Phys.* **97**, 8811 (1992).

<sup>10</sup>Z. Hu, J.-G. Dong, J. R. Lombardi, and D. M. Lindsay, *J. Phys. Chem.* **97**, 9263 (1993).

<sup>11</sup>D. G. Leopold, T. M. Miller, and W. C. Lineberger, *J. Am. Chem. Soc.* **108**, 178 (1986).

<sup>12</sup>M. Morse, *Chem. Rev.* **86**, 1049 (1986).

<sup>13</sup>W. Harbich, S. Fedrigo, F. Meyer, D. M. Lindsay, J. Lignieres, J. C. Rivoal, and D. Kreisler, *J. Chem. Phys.* **93**, 8535 (1990).

<sup>14</sup>Since the diode detector AR coated at 900 nm was not received until after most spectroscopic measurements were already made.

<sup>15</sup>Product of current and deposition time in hours; 1 nA h =  $2.25 \times 10^{13}$  particles.

<sup>16</sup>Wavelengths in this paper pertain to measurements in air, whereas energies are given in vacuum wave numbers.

<sup>17</sup>G. Herzberg, *Spectra of Diatomic Molecules* (Van Nostrand, New York, 1950).

<sup>18</sup>The pertinent expressions are:  $k = 2\sigma^2 D_e$ ,  $\beta = -\sigma^3 D_e$ , and  $\gamma = 7/12 \sigma^4 D_e$  plus the additional relation  $D_e = \omega_e^2/4 \omega_e x_e$ . These formulas may be obtained by comparing derivatives of the Morse function,  $V(x) = D_e \{1 - \exp[-\sigma(x - x_e)]\}^2$  and the Taylor series expansion  $V(x) = 0.5k(x - x_e)^2 + \beta(x - x_e)^3 + \gamma(x - x_e)^4$ .

<sup>19</sup>Formula 2 in paragraph 3.462 of I. S. Gradshteyn and I. M. Ryzhik, *Tables of Integrals, Series and Products* (Academic, New York, 1965).

<sup>20</sup>The X and D states of  $C_2$ , for example, have  $r_e' = 1.242 \text{ \AA}$  and  $r_e'' = 1.238 \text{ \AA}$  with  $\omega_e' = 1855 \text{ cm}^{-1}$  but  $\omega_e'' = 1830 \text{ cm}^{-1}$ . See Ref. 17.

<sup>21</sup>See, for example, R. W. Nicholls, *Proc. Phys. Soc.* **69**, 741 (1956).

<sup>22</sup>A. R. Gee, D. C. O'Shea, and H. Z. Cummins, *Solid State Commun.* **4**, 43 (1965).

<sup>23</sup>M. Morse, private communication.

<sup>24</sup>S. P. Walch and C. W. Bauschlicher, in *Comparison of Ab Initio Quantum Chemistry with Experiment*, edited by R. J. Bartlett (Reidel, Boston, 1985).

<sup>25</sup>M. D. Morse, *Adv. Metal Semicond. Clusters* **1**, 1 (1992).

<sup>26</sup>An interesting counter example (but not in the context of transition metal dimers) is  $N_2$  whose  $X(^1\Sigma_g^+)$  state correlates smoothly with the atomic  $s^2 p^3 + s^2 p^3$  asymptote. See F. R. Gilmore, *Potential Energy Curves for  $N_2$ , NO,  $O_2$  and Corresponding Ions* (Rand Corp. memorandum R-4034-PR, 1964).

<sup>27</sup>C. E. Moore, *Atomic Energy Levels*, Natl. Stand. Ref. Data Ser. No. 35 (U.S. Natl. Bur. Stand., Washington, DC, 1971). The position of  $5d^6 4s^1$  levels was determined by "subtracting out" the spin-orbit splitting of the  $^6D_J$  levels using the Landé interval rule, which was also gives  $\zeta(^6D) \approx -500 \text{ cm}^{-1}$ , so that  $\zeta_{5d} = -5\zeta(^6D) \approx 2500 \text{ cm}^{-1}$ . See M. Tinkham, *Group Theory and Quantum Mechanics* (McGraw-Hill, New York, 1964).

<sup>28</sup>Although more complicated arrangements such as  $s\sigma_g^2 d\sigma_g^2 d\pi_u^4 d\delta_g^2 s\sigma_u d\delta_u^2$  cannot be ruled out, certain transitions such as  $d\delta_g^4 s\sigma_u^2 \leftarrow d\delta_g^3 s\sigma_u d\delta_u^2$  involve two electrons and so would be quite unlikely.

<sup>29</sup>H. Lefebvre-Brion and R. W. Field, *Perturbations in the Spectra of Diatomic Molecules* (Academic, New York, 1986).

<sup>30</sup>L. Pauling, *The Nature of the Chemical Bond* (Cornell University, Ithaca, NY, 1960).

<sup>31</sup>H. S. Johnston, *Gas Phase Reaction Rate Theory* (Ronald, New York, 1966).

<sup>32</sup>Computed from  $V(r) = (I - E) + 14.4/r$ , where  $I = 7.87 \text{ eV}$  is the ionization potential (Ref. 27) and  $E = 0.15 \text{ eV}$  the atomic electron affinity. See H. Hotop and W. C. Lineberger, *J. Phys. Chem. Ref. Data* **4**, 539 (1975).

<sup>33</sup>See Table I of Ref. 10. Note that the force constant given for  $Re_2$  (6.66 mdyne/ $\text{\AA}$ ) is too large and should be replaced by the 6.26 mdyne/ $\text{\AA}$  value reported here.

<sup>34</sup>C. A. Baumann, R. J. Van Zee, S. V. Bhat, and W. Weltner, *J. Chem. Phys.* **78**, 190 (1983); M. Cheeseman, R. J. Van Zee and W. Weltner, *ibid.* **91**, 2748 (1989).

<sup>35</sup>K. D. Bier, T. L. Haslett, A. D. Kirkwood, and M. Moskovits, *J. Chem. Phys.* **89**, 6 (1988); T. L. Haslett, M. Moskovits, and A. L. Weitzman, *J. Molec. Spectrosc.* **135**, 259 (1989).

<sup>36</sup>R. K. Nesbitt, *Phys. Rev. A* **135**, 460 (1964).

<sup>37</sup>Data from Table I of C. Kittel, *Introduction to Solid State Physics* (Wiley, New York, 1976).